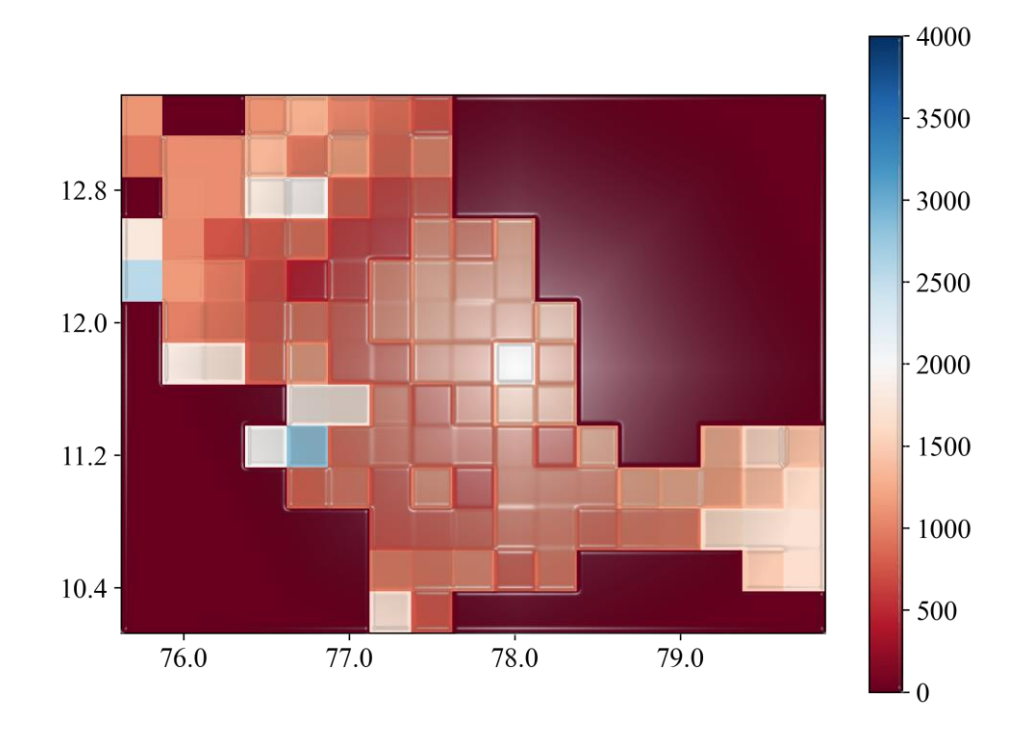


National River Conservation Directorate

Ministry of Jal Shakti, Department of Water Resources, River Development and Ganga Rejuvenation Government of India

Climatological/Meteorological Data Cauvery Basin



March 2025





© cCauvery, cGanga and NRCD, 2024



Climatological/Meteorological Data Cauvery Basin





© cCauvery, cGanga and NRCD, 2024

National River Conservation Directorate (NRCD)

The National River Conservation Directorate, functioning under the Department of Water Resources, River Development and Ganga Rejuvenation, and Ministry of Jal Shakti providing financial assistance to the State Government for conservation of rivers under the Centrally Sponsored Schemes of 'National River Conservation Plan (NRCP)'. National River Conservation Plan to the State Governments/ local bodies to set up infrastructure for pollution abatement of rivers in identified polluted river stretches based on proposals received from the State Governments/ local bodies.

www.nrcd.nic.in

Centres for Cauvery River Basin Management Studies (cCauvery)

The Centre for Cauvery River Management Studies (cCauvery) is a Brain Trust dedicated to River Science and River Basin Management. Established in 2024 by IISc Bengaluru and NIT Tiruchirappalli, under the supervision of cGanga at IIT Kanpur, the centre serves as a knowledge wing of the National River Conservation Directorate (NRCD). cCauvery is committed to restoring and conserving the Cauvery River and its resources through the collation of information and knowledge, research and development, planning, monitoring, education, advocacy, and stakeholder engagement.

www.ccauvery.org

Centre for Ganga River Basin Management and Studies (cGanga)

cGanga is a think tank formed under the aegis of NMCG, and one of its stated objectives is to make India a world leader in river and water science. The Centre is headquartered at IIT Kanpur and has representation from most leading science and technological institutes of the country. cGanga's mandate is to serve as think-tank in implementation and dynamic evolution of Ganga River Basin Management Plan (GRBMP) prepared by the Consortium of 7 IITs. In addition to this, it is also responsible for introducing new technologies, innovations, and solutions into India.

www.cganga.org

Acknowledgment

This report is a comprehensive outcome of the project jointly executed by IISc Bengaluru (Lead Institute) and NIT Tiruchirappalli (Fellow Institute) under the supervision of cGanga at IIT Kanpur. It was submitted to the National River Conservation Directorate (NRCD) in 2024. We gratefully acknowledge the individuals who provided information and photographs for this report.

Disclaimer

This report is a preliminary version prepared as part of the ongoing Condition Assessment and Management Plan (CAMP) project. The analyses, interpretations and data presented in the report are subject to further validation and revision. Certain datasets or assessments may contain provisional or incomplete information, which will be updated and refined in the final version of the report after comprehensive review and verification.

Team

Praveen C Ramamurthy, cCauvery, IISc Bengaluru Shekhar M, cCauvery, IISc Bengaluru Nagesh Kumar Dasika, cCauvery, IISc Bengaluru Srinivas V V, cCauvery, IISc Bengaluru Lakshminarayana Rao, cCauvery, IISc Bengaluru Rajarshi Das Bhowmik, cCauvery, IISc Bengaluru Bramha Dutt Vishwakarma, cCauvery, IISc Bengaluru Debsunder Dutta, cCauvery, IISc Bengaluru R Manjula, cCauvery, NIT Trichy Nisha Radhakrishnan, cCauvery, NIT Trichy S Saravanan, cCauvery, NIT Trichy Aneesh Mathew, cCauvery, NIT Trichy Laveti Satish, cCauvery, NIT Trichy Prabu P, cCauvery, NIT Trichy Dr Vinod Tare, cGanga, IIT Kanpur

Preface

In an era of unprecedented environmental change, understanding our rivers and their ecosystems has never been more critical. This report aims to provide a comprehensive overview of our rivers, highlighting their importance, current health, and the challenges they face. As we explore the various facets of river systems, we aim to equip readers with the knowledge necessary to appreciate and protect these vital waterways.

Throughout the following pages, you will find an in-depth analysis of the principles and practices that support healthy river ecosystems. Our team of experts has meticulously compiled data, case studies, and testimonials to illustrate the significant impact of rivers on both natural environments and human communities. By sharing these insights, we hope to inspire and empower our readers to engage in river conservation efforts.

This report is not merely a collection of statistics and theories; it is a call to action. We urge all stakeholders to recognize the value of our rivers and to take proactive steps to ensure their preservation. Whether you are an environmental professional, a policy maker, or simply someone who cares about our planet, this guide is designed to support you in your efforts to protect our rivers.

We extend our heartfelt gratitude to the numerous contributors who have generously shared their stories and expertise. Their invaluable input has enriched this report, making it a beacon of knowledge and a practical resource for all who read it. It is our hope that this report will serve as a catalyst for positive environmental action, fostering a culture of stewardship that benefits both current and future generations.

As you delve into this overview of our rivers, we invite you to embrace the opportunities and challenges that lie ahead. Together, we can ensure that our rivers continue to thrive and sustain life for generations to come.

Centres for Cauvery River Basin Management and Studies (cCauvery) IISc Bengaluru (Lead Institute), NIT Tiruchirappalli (Fellow Institute)



Contents

Preface	V
List of Figures	viii
List of Tables	ix
Abbreviations and Acronyms	xi
1. Introduction	1 - 2
2. Datasets used	3-6
3. Spatiotemporal variations of meteorological variables	7 - 11
3.1. Annual rainfall	7-8
3.2. Annual minimum temperature	8-9
3.3. Annual maximum temperature	10-11
4. Historical trends	11-14
4.1. Basin-averaged annual rainfall	11-12
4.2. Basin-averaged annual minimum temperature	12-13
4.3. Basin-averaged annual maximum temperature	13-14
5. Decadal variations	15-17
5.1. Decadal mean rainfall	15
5.2. Decadal mean minimum temperature	16
5.3. Decadal mean maximum temperature	17
6. Monthly relative humidity variability across different stations	18-19
7. Monthly evaporation variability across different stations	19-20
8. Monthly wind velocity variability across different stations	21-22
9. Bias-corrected climate projections from CMIP6 models	23-27
9.1. Rainfall future projections	23-25
9.2. Minimum temperature future projections	25-26
9.3. Maximum temperature future projections	26-27
10. Past drought & flood incidents in the CRB	27-28
11. Summary and recommendations	29-30
12. Significance of the climatological profile of the CRB	30
References	30-32

List of Figures

Fig. 1.	Spatial distribution of meteorological stations within the CRB	7
Fig. 2.	Spatial distribution of annual rainfall (mm) over the CRB from IMD data (0.25°) . Annual rainfall represents the daily rainfall summed for each grid cell for a given year	8
Fig. 3.	Spatial distribution of annual minimum temperature (°C) over the CRB from IMD data (0.25°). Annual minimum temperature represents the mean of daily minimum temperatures for each grid cell for a given year	9
Fig. 4.	Spatial distribution of annual maximum temperature (°C) over the CRB from IMD data (0.25°). Annual maximum temperature represents the mean of daily maximum temperatures for each grid cell for a given year	10
Fig. 5.	Time-series of basin-averaged annual rainfall (mm) from 1951-2024	12
Fig. 6.	Time-series of basin-averaged annual minimum temperature (°C) from 1951-2024	13
Fig. 7.	Time-series of basin-averaged annual maximum temperature (°C) from 1951-2024	14
Fig. 8.	Decadal mean rainfall variations in the CRB (1951-2020)	15
Fig. 9.	Decadal mean minimum temperature variations in the CRB (1951-2020)	16
Fig. 10.	Decadal mean maximum temperature variations in the CRB (1951-2020)	17
Fig. 11.	Monthly variation of relative humidity (%) at selected CWC stations across the CRB (stream names in brackets)	18
Fig. 12.	Monthly variation of evaporation (mm) at selected CWC stations across the CRB (stream names in brackets)	20
Fig. 13.	Monthly variation of wind velocity (km/h) at selected CWC stations across the CRB (stream names in brackets)	22
Fig. 14.	Ensemble mean of annual rainfall (2015-2100) over the CRB under various bias-corrected CMIP6 SSP scenarios	24
Fig. 15.	Ensemble mean of annual minimum temperature (2015-2100) over the CRB under various bias-corrected CMIP6 SSP scenarios	25
Fig. 16.	Ensemble mean of annual maximum temperature (2015-2100) over the CRB under various bias-corrected CMIP6 SSP scenarios	27

List of Tables

Table 1. Dataset characteristics and their relevance to the CRB	2
Table 2. Description of models used for future climate projections	23



Abbreviations and Acronyms

° Degree

°C Degree Celsius

hPa Hectopascal

h Hour

km Kilometre

mm Millimetre

' Minute

% Percentage

CWC Central Water Commission

CMIP6 Coupled Model Intercomparison Project Phase 6

CRB Cauvery River Basin

EC-Earth3 European Community Earth System Model version 3

IMD India Meteorological Department

MPI Max Planck Institute for Meteorology

MPI-ESM1-2-HR Max Planck Institute Earth System Model, version 1.2 - High

Resolution

MRI Meteorological Research Institute

MRI-ESM2-0 Meteorological Research Institute Earth System Model version 2.0

NE Northeast

SSP Shared Socioeconomic Pathway

SW Southwest

1. Introduction

The Cauvery River Basin (CRB) exhibits a predominantly tropical to sub-tropical climate, shaped largely by the seasonal monsoon systems. The basin experiences four distinct seasons- winter (January-February), summer (March-May), the southwest (SW) monsoon (June-September), and the northeast (NE) monsoon (October-December) (Cauvery Basin Report, Department of Space & Ministry of Water Resources, Government of India). Considerable spatial climatic variability arises from the basin's contrasting physiographic settings, which range from the high-relief Western Ghats to the semi-arid plains of Karnataka and Tamil Nadu.

Rainfall across the basin is monsoon-dominated. The SW monsoon delivers the bulk of annual precipitation to the upstream regions of Karnataka and Kerala (Gouda et al., 2024), while the NE monsoon forms the principal rainfall source for Tamil Nadu and the deltaic tracts (SK et al., 2023). Orographic uplift along the Western Ghats produces intense rainfall in the upper catchments, where the Cauvery and several major tributaries originate. The mountainous belts of the Western Ghats and the Nilgiris thus receive the highest annual rainfall. In contrast, the plateau and rolling uplands downstream lie in the rain-shadow zone, resulting in markedly reduced rainfall. Toward the delta, rainfall increases again due to the strong influence of the NE monsoon (Ghosh et al., 2018).

Based on the India Meteorological Department (IMD) gridded climatology (1951-2024), the mean maximum and minimum temperatures over the basin are 31.64°C and 19.57°C, respectively. Temperature variability is relatively moderate in the Western Ghats but increases toward the interior plateau and the eastern plains, where higher extremes are observed.

Rainfall distribution is highly heterogeneous, reflecting both monsoonal flow patterns and topographic controls. IMD rainfall data (1951-2024) show that annual rainfall over the basin ranges from approximately 207 mm in the semi-arid interior regions to about 873 mm in the high-rainfall zones of the Western Ghats, illustrating strong spatial gradients and considerable interannual variability. Climatically, the basin transitions from pre-humid conditions in the far north-western part to humid, moist sub-humid, dry sub-humid, and semi-arid zones moving eastward. The region is also periodically influenced by Bay of

Bengal depressions and cyclonic systems, which produce intense rainfall episodes during the post-monsoon period.

The CRB is heavily dependent on monsoon rainfall and becomes highly vulnerable to droughts when monsoon failures occur. Large parts of the basin, particularly the interior plains, fall within the dry sub-humid to semi-arid categories (Sushant et al., 2015). The basin spans three major agro-climatic zones: the West Coast Plains and Ghats, the East Coast Plains and Hills, and the Southern Plateau and Hills. A significant portion lies within the Southern Plateau and Hills zone, characterized by comparatively low rainfall and frequent drought occurrence.

Overall, the climatology of the CRB reflects complex interactions among monsoon dynamics, topography, and synoptic-scale disturbances, resulting in pronounced spatiotemporal variability in rainfall and temperature patterns. In this report, a comprehensive assessment of CRB climatological characteristics is carried out using longterm observational datasets spanning 1951-2024, covering key variables such as rainfall, minimum temperature, and maximum temperature. Beyond characterizing historical variability and trends, the analysis is extended to future climate conditions using biascorrected future projections of Coupled Model Intercomparison Project Phase 6 (CMIP6) models, namely European Community Earth System Model version 3 (EC-Earth3), Max Planck Institute Earth System Model, version 1.2- High Resolution (MPI-ESM1-2-HR), Meteorological Research Institute Earth System Model version 2.0 (MRI-ESM2-0) selected for their strong performance in simulating the Indian Summer Monsoon and regional hydroclimatic dynamics. The bias-corrected future projections follow the Empirical Quantile Mapping (EQM) approach, and the datasets were downloaded from Mishra et al. (2020). Future climate evolution is evaluated under four Shared Socioeconomic Pathways (SSP126, SSP245, SSP370, and SSP585) to assess potential changes in rainfall regimes and temperature trajectories. Together, the historical analyses and model-based projections provide an integrated understanding of past climate behaviour and likely future shifts, offering essential insights for informed water resource management and climate-resilient planning within the CRB.

2. Datasets used

A range of meteorological variables was compiled to assess long-term variability in the CRB, the details of which are mentioned in Table 1.

Table 1. Dataset characteristics and their relevance to the CRB

S. No.	Variable (units)	Source	Resolution/ Stations	Time period	Importance
1	Daily rainfall (mm)	IMD	0.25°	1951-2024	Detecting long-term trends, monsoon variability, and drought patterns
2	Daily minimum and maximum temperatur es (°C)	IMD	0.5°	1951-2024	Important for evaluating evapotranspiration, groundwater recharge potential, heatwave occurrence, drought intensification, crop stress, land—atmosphere interactions, and long-term warming signals
3	Daily relative humidity (%)	CWC	Akkihebbal (Hemavathi), Annavasal (Nattar), Biligundulu (Cauvery), Elunuthimangalam (Noyyal), Gopurajapuram	2012-2022	Key atmospheric variable that regulates evapotranspiration, soil-plant-

			(Puravidayanar), K.M. Vadi (Lakshmanathirtha), Kodumudi (Cauvery), Kollegal (Cauvery), Kudige (Cauvery), Kudlur (Palar), M.H. Halli (Hemavathi), Menangudi (Noolar), Musiri (Cauvery), Nallathur (Nandalar), Nellithurai (Bhavani), Peralam (Vanjiyar), Porakudi (Arasalar), Sakleshpur (Hemavathi), Sevanur (Chittar), T. Narsipur (Kabini), Thengudi (Thirumalairajanar), Thengumarahada (Moyar), Thevur (Sarabenga), Urachikottai		atmosphere moisture exchange, monsoon dynamics, and boundary-layer processes
			(Cauvery)		
4	Daily evaporatio n (mm)	CWC	Akkihebbal (Hemavathi), Annavasal (Nattar), Biligundulu (Cauvery), Elunuthimangalam (Noyyal), Kodumudi (Cauvery), Kollegal (Cauvery), Kudige (Cauvery), M.H. Halli (Hemavathi), Musiri (Cauvery),	2012-2022	Major component of the hydrological cycle governing surface-water losses from reservoirs, tanks, soils, and crops. Directly influences groundwater recharge, irrigation

			Nallamaranpathy (Amaravathy), Nellithurai (Bhavani), Peralam (Vanjiyar), Porakudi (Arasalar), Sakleshpur (Hemavathi), Savandapur (Bhavani), T. Narsipur (Kabini), Thengudi (Thirumalairajanar), Urachikottai (Cauvery)		demand, reservoir storage behaviour, and water balance modelling
5	Daily wind velocity (km/h)	CWC	Akkihebbal (Hemavathi), Annavasal (Nattar), Biligundulu (Cauvery), Elunuthimangalam (Noyyal), Gopurajapuram (Puravidayanar), K.M. Vadi (Lakshmanathirtha), Kodumudi (Cauvery), Kollegal (Cauvery), Kudige (Cauvery), Kudlur (Palar), M.H. Halli (Hemavathi), Menangudi (Noolar), Musiri (Cauvery), Muthankera (Kabini), Nallamaranpathy (Amaravathy), Nallathur (Nandalar), Nellithurai (Bhavani), Peralam (Vanjiyar), Porakudi (Arasalar), Sakleshpur	2012-2022	Controls evaporation rates, moisture transport, and monsoon circulation patterns

			(Hemavathi), Savandapur (Bhavani), Sevanur (Chittar), T.Bekuppe (Arkavathi), T.Narsipur (Kabini), Thengudi (Thirumalairajanar), Thengumarahada (Moyar), Thevur (Sarabenga), Thoppur (Thoppaiyar), Urachikottai (Cauvery)		
6	Bias-	Couple	0.25°	2015-2100	Provide insight into
	corrected	d			how rainfall patterns,
	future	Model			temperature regimes,
	projection	Interco			extremes, and
	s of daily	mpariso			monsoon
	rainfall,	n			characteristics may
	minimum,	Project			evolve in the future
	and	Phase 6			under different
	maximum	(CMIP			Shared
	temperatur	6),			Socioeconomic
	e	Mishra			Pathway (SSP)-
		et al.			SSP126, SSP245,
		(2020)			SSP370, SSP585
1		I			1

The geographical distribution of the 54 CWC meteorological stations across the entire CRB is shown in Fig. 1. The stations are well distributed from the high-rainfall Western Ghats through the central plains to the lower deltaic region, providing comprehensive coverage of the basin's diverse hydro-climatic settings. The inset map offers a detailed view of the cluster of stations located in the eastern coastal districts of Tamil Nadu.

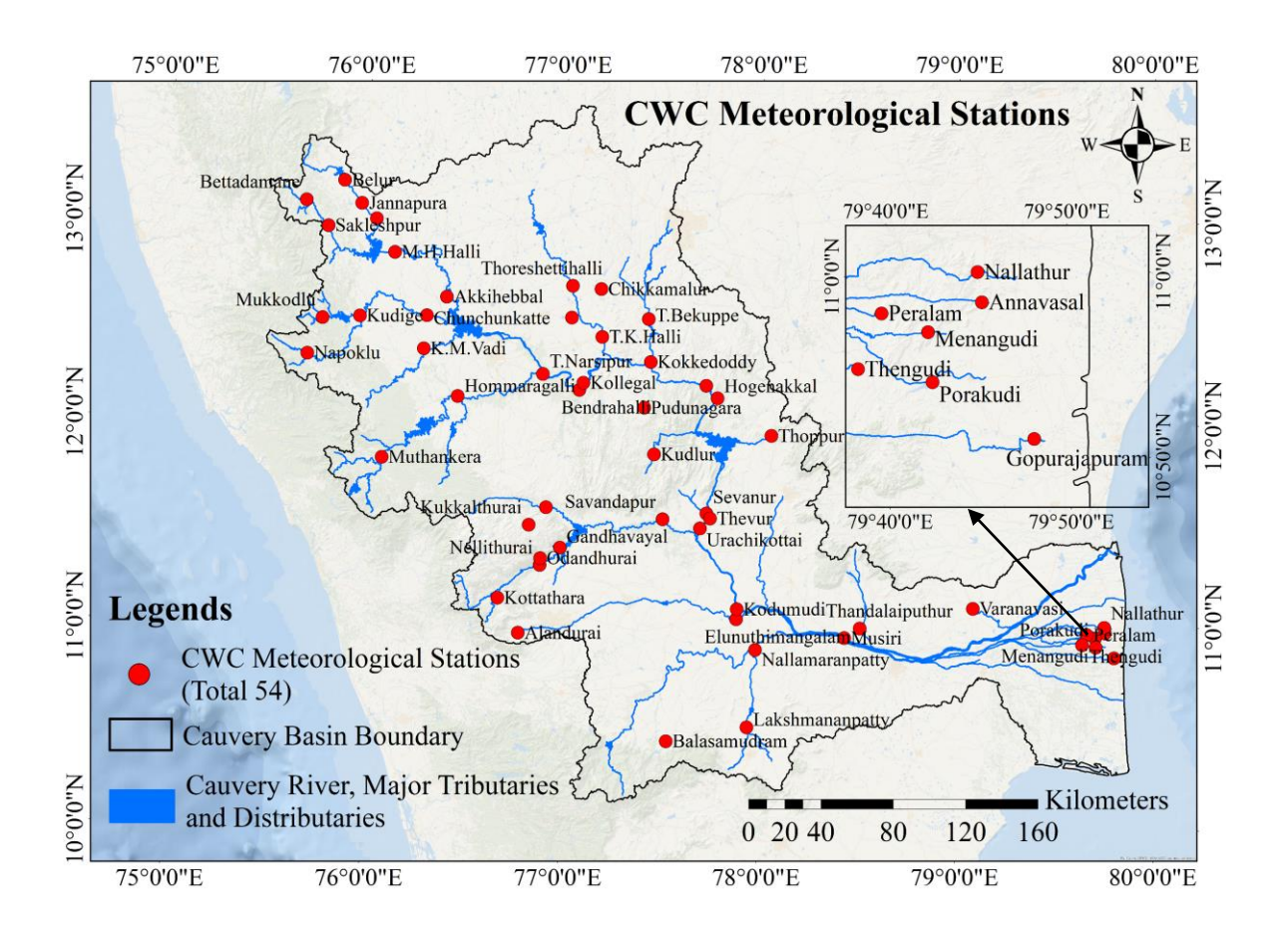


Fig. 1. Spatial distribution of meteorological stations within the CRB

3. Spatiotemporal variations of meteorological variables

3.1. Annual rainfall

Daily rainfall data at 0.25° spatial resolution from the IMD for the period 1951-2024 were used to analyse long-term hydroclimatic variability in the CRB. Annual rainfall totals for each grid cell were derived from the daily dataset, hereafter referred to as "annual rainfall." Although annual rainfall maps were generated for all years, only selected years are presented in Fig. 2 for clarity.

Fig. 2 presents spatial maps of annual rainfall for selected years at decadal intervals (1954, 1964, 1974, 1984, 1994, 2004, 2014, and 2024), highlighting clear spatial contrasts in rainfall distribution across the basin. In all years, the highest rainfall occurs in the western part of the CRB, particularly along the foothills of the Western Ghats, and gradually decreases toward the eastern and southeastern regions. This persistent west-to-east gradient reflects strong

orographic uplift induced by the Western Ghats, which enhances rainfall on the windward side while creating a pronounced rain-shadow zone toward the interior Tamil Nadu region.

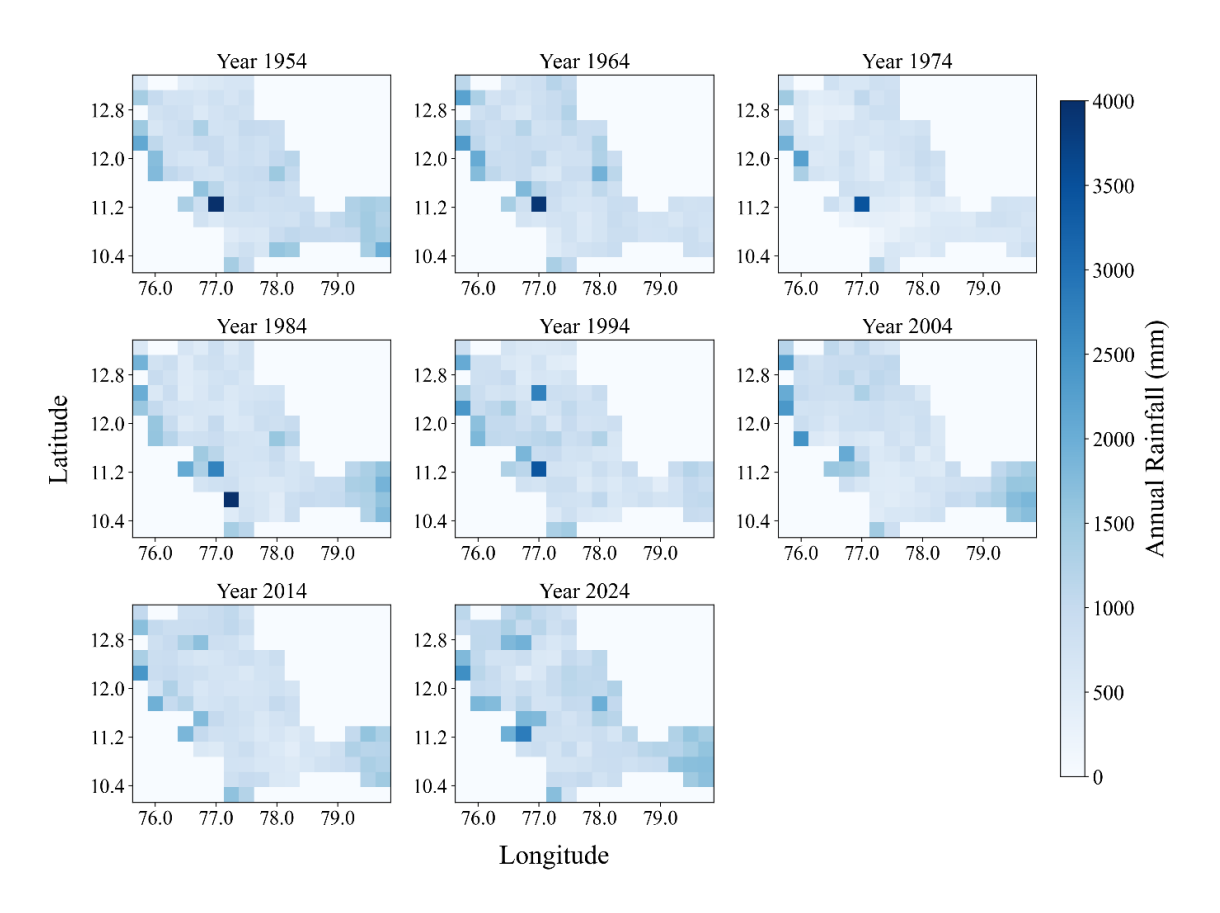


Fig. 2. Spatial distribution of annual rainfall (mm) over the CRB from IMD data (0.25°). Annual rainfall represents the daily rainfall summed for each grid cell for a given year

3.2. Annual minimum temperature

Daily minimum temperature data from IMD (0.5° resolution) for the period 1951-2024 was used to compute the average minimum temperature for each grid cell for every year. This annual average is hereafter referred to as the "annual minimum temperature." These annual minimum temperature maps were generated for every year in the study period; however, spatial panels for only selected years between 1954 and 2024 are shown in Fig. 3. These selected panels highlight the long-term warming pattern evident across the 70-year period. Early years such as 1954, 1964, 1974, 1984, 1994, and 2004 predominantly display dark blue shades, indicating cooler minimum temperatures. However, as the timeline progresses toward 2014 and 2024, these cooler regions (dark blue) gradually fade, reflecting a steady rise in minimum temperatures across the region.

Despite this overall warming, the spatial distribution of temperatures remains broadly consistent. The northwestern part of the region remains relatively cooler throughout, while the southeastern part consistently exhibits higher minimum temperatures. This indicates that although warming occurs across the entire domain, the underlying spatial temperature gradient remains largely unchanged. By 2014 and 2024, the southeastern areas display deep red shades, representing the warmest minimum temperatures in the dataset, consistent with the accelerated warming observed globally since the late twentieth century.

The southeastern region, particularly around longitudes 78-79.2°, exhibits the most dramatic increase in minimum temperatures. These emerging hotspots may be influenced by factors such as urbanization, land-use changes, or regional climatic shifts. This localized intensification suggests that certain areas are warming faster than the surrounding region.

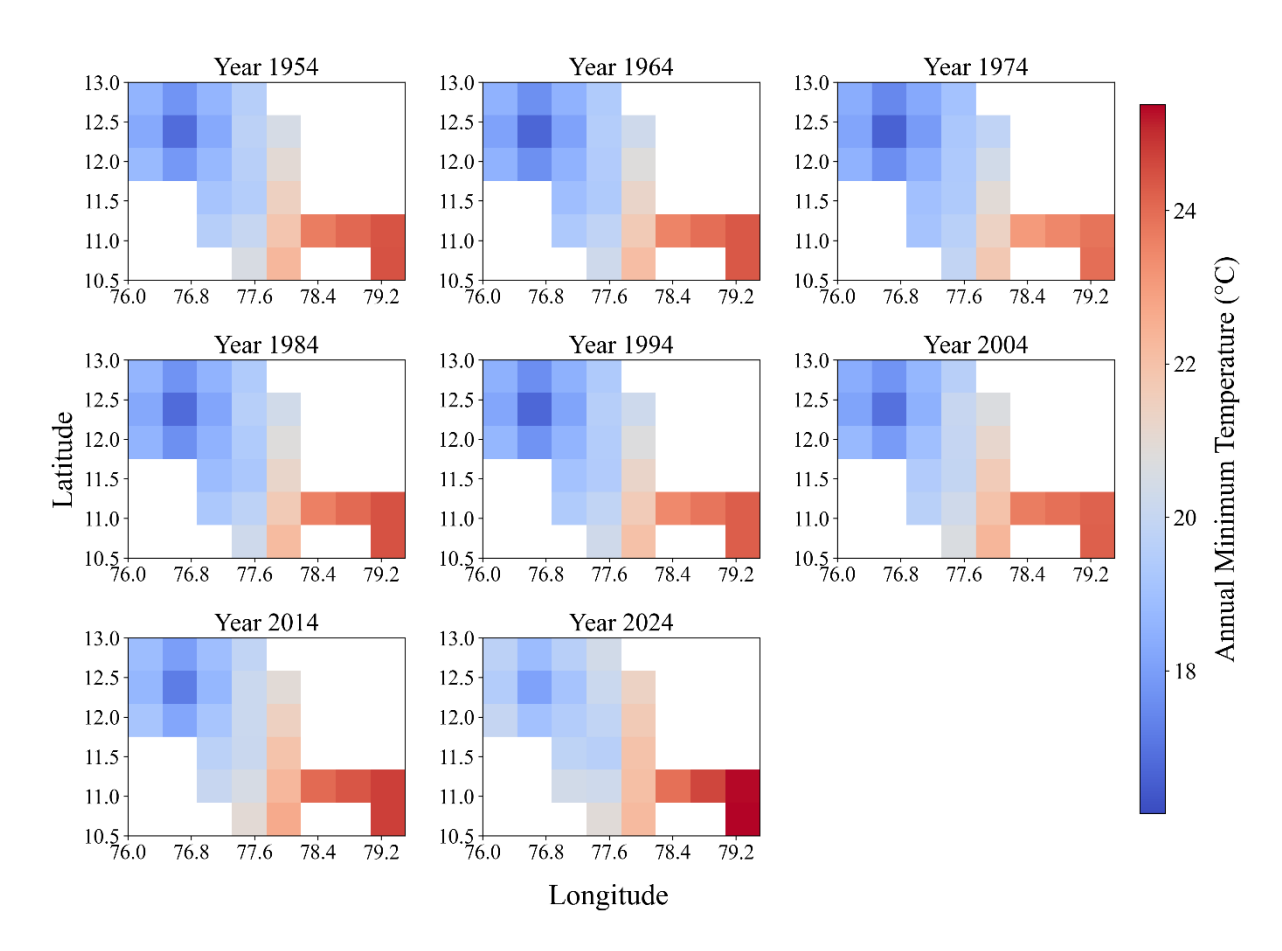


Fig. 3. Spatial distribution of annual minimum temperature (°C) over the CRB from IMD data (0.25°). Annual minimum temperature represents the mean of daily minimum temperatures for each grid cell for a given year

3.3. Annual maximum temperature

Daily maximum temperature data from IMD (0.5° resolution) was used to calculate the average maximum temperature for each grid cell for every year. This annual average maximum temperature is hereafter referred to as the "annual maximum temperature." These annual maximum temperature values were generated for each year from 1951-2024. Although annual maps were produced for the entire study period, spatial panels are presented only for selected years between 1954 and 2024 to illustrate long-term variability (Fig. 4).

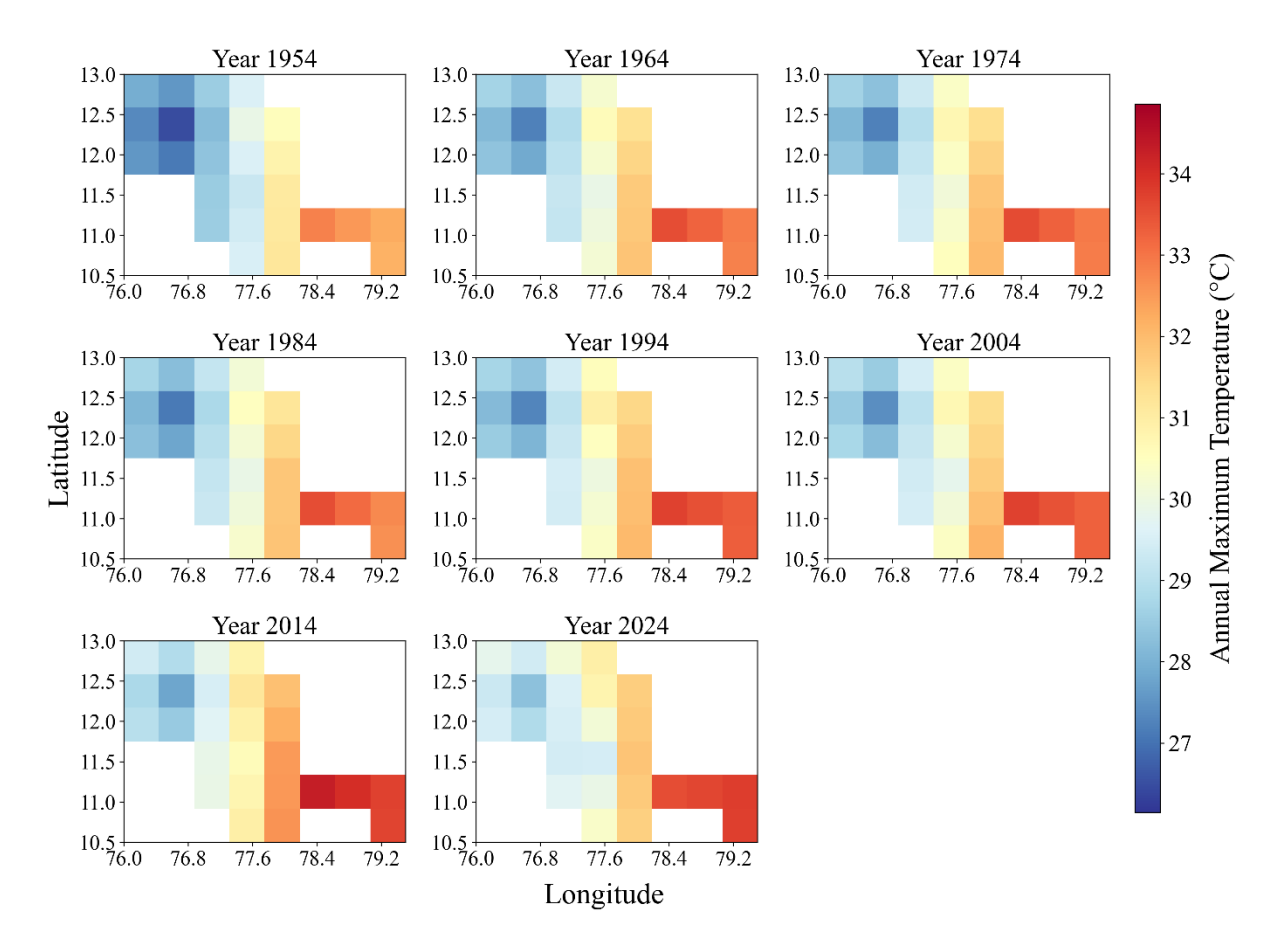


Fig. 4. Spatial distribution of annual maximum temperature (°C) over the CRB from IMD data (0.25°). Annual maximum temperature represents the mean of daily maximum temperatures for each grid cell for a given year

The spatial distribution reveals a clear and consistent warming trend across the basin. In 1954, cooler temperature classes (dark blue) appear prominently, particularly over the northern and central regions. Over the following decades, the dominance of these cooler classes gradually weakens, with a noticeable fading of blue shades from 2004 onward. At

the same time, beginning around 1994, warmer temperature classes (yellow to red) increasingly intensify, becoming more prominent toward the southern and southeastern parts of the basin. From 2004 onward, a marked intensification of high-temperature zones is evident, with the 2014 and 2024 panels showing widespread warming and the emergence of persistent hotspots in the southeastern region.

This progression indicates a consistent shift toward higher maximum temperatures over the years, reflecting long-term warming likely linked to regional climate change. The spatial contrast between cooler northern portions and warmer southern portions remains evident but becomes increasingly skewed toward warmer temperature classes over time.

Overall, these patterns demonstrate both temporal warming and spatial amplification of maximum temperatures, with the most pronounced heating observed in recent decades.

4. Historical trends

4.1. Basin-averaged annual rainfall

From the annual sum rainfall, basin-wide averages were computed to obtain a single representative value for each year, hereafter referred to as "basin-averaged annual rainfall." The Mann-Kendall test for basin-averaged annual rainfall yields a p-value of 0.03 and a Kendall's Tau of 0.17, indicating a weak but statistically significant positive monotonic trend during the period 1951-2024. The fitted trend line reflects a gradual long-term increase in basin-averaged annual rainfall, consistent with the weak increasing tendency (Fig. 5). Despite this positive trend, the basin-averaged annual series exhibits substantial interannual variability, with fluctuations occurring throughout the seven decades. Several high-rainfall years-particularly after the mid-2000s-stand out, while anomalously low rainfall years, especially around the early 2000s, highlight periods of deficit. In recent decades, variability has become more pronounced, characterized by both extremely high and extremely low annual totals. The clustering of wetter years in the post-2000 period contributes to the overall upward trend, even though decadal mean rainfall still fluctuates within a relatively narrow band of approximately 450-500 mm. Together, these patterns suggest that while long-term rainfall is increasing modestly, the system is also experiencing greater year-to-year volatility, a combination that has important implications for water resource management, hydrological planning, and climate adaptation under a changing climate.

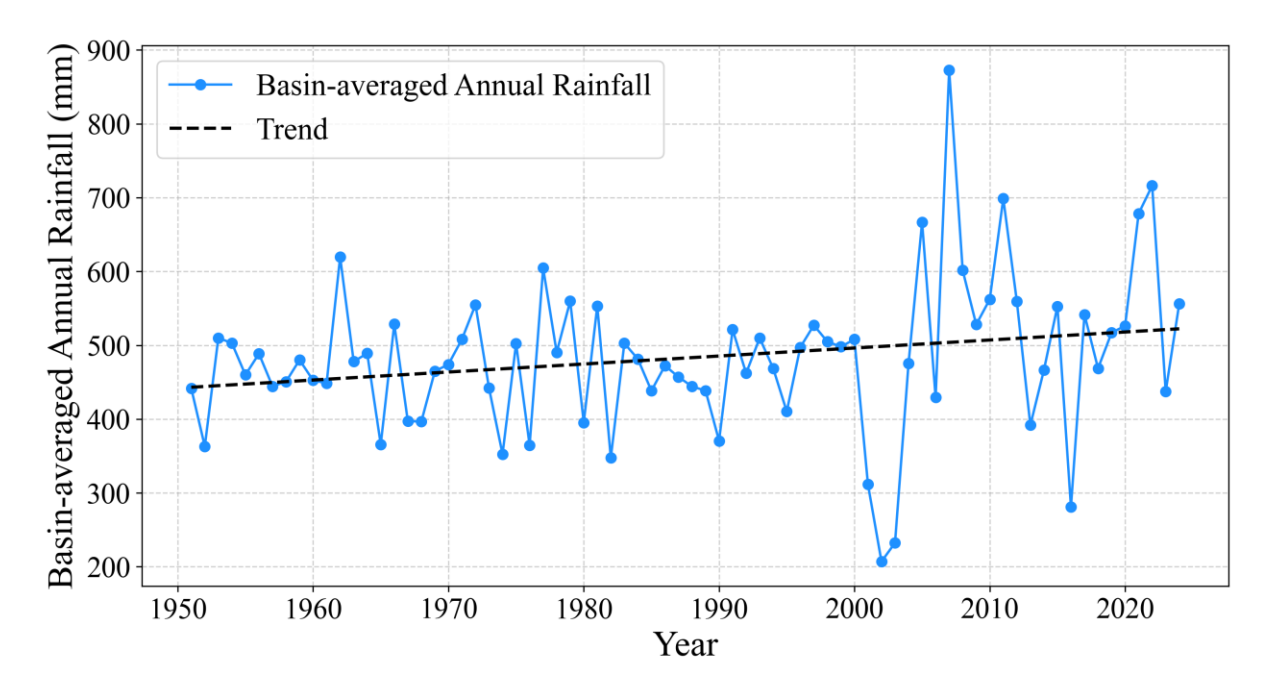


Fig. 5. Time-series of basin-averaged annual rainfall (mm) from 1951-2024

4.2. Basin-averaged annual minimum temperature

Annual minimum temperature values were averaged across all grid cells, producing a single annual value referred to as the "basin-averaged annual minimum temperature." Fig. 6 presents the temporal variation of this metric from 1951-2024. The Mann-Kendall trend test applied to this time series reveals a statistically significant upward trend, with a p-value of 0.00 indicating an exceptionally high level of confidence in the result. Additionally, the positive Kendall's Tau value of 0.39 signifies a moderate but consistent increase in the basin-averaged annual minimum temperature over the 70-year period.

During the earlier decades, particularly between the 1951 and 1995, the annual minimum temperatures show substantial interannual variability. Temperatures fluctuate frequently, with several years dipping below 20°C. Despite this variability, the overall tendency during this period is relatively cooler compared to later decades. After 1995, minimum temperature begin to show a clearer upward shift. Although variability continues, the lower values seen in earlier decades become increasingly rare. In the most recent decades, particularly after 2011, the warming becomes more pronounced. Annual minimum temperatures frequently exceed 21°C, and several years stand out as among the warmest in the entire record. The

upward trajectory in this period is steep, indicating accelerated warming consistent with broader climate change signals in many regions. The peak value observed in 2019 highlights that minimum temperatures now regularly reach levels significantly higher than those recorded at the beginning of the observation period.

The strong statistical significance of the Mann-Kendall test confirms that the observed increase in minimum temperatures is robust and highly unlikely to be the result of random natural fluctuations.

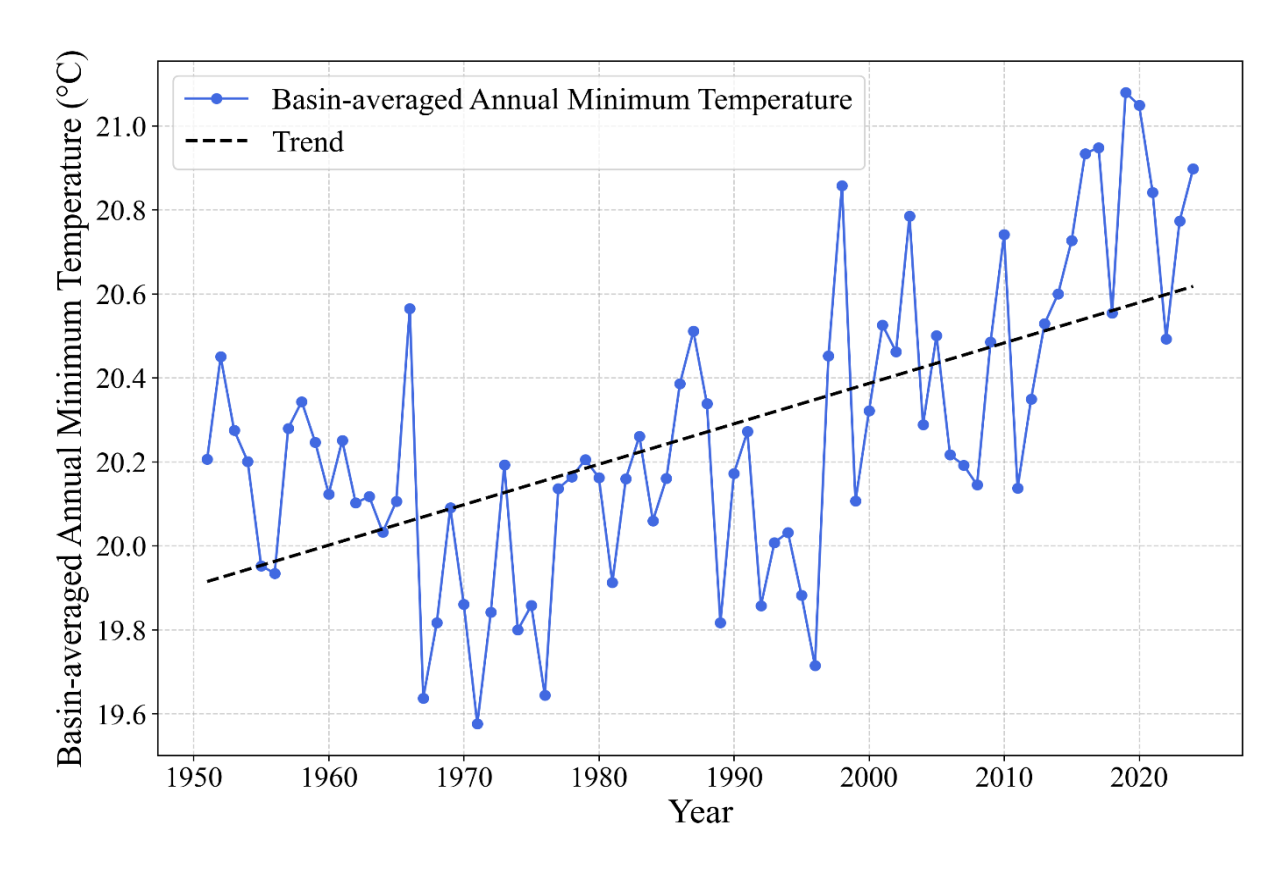


Fig. 6. Time-series of basin-averaged annual minimum temperature (°C) from 1951-2024

4.3. Basin-averaged annual maximum temperature

To represent the thermal conditions of the entire basin, the annual maximum temperature values were spatially averaged across all grid cells, resulting in a single annual value for each year, hereafter termed the "basin-averaged annual maximum temperature." The time series of basin-averaged annual maximum temperature from 1951-2024 shows a strong and statistically significant warming trend across the CRB (Fig. 7). The Mann-Kendall test yields p = 0.00 and Tau = 0.59, indicating a highly significant and moderately strong

positive monotonic trend. This confirms that maximum temperatures have been rising consistently over the 74-year period.

The plotted temperature values exhibit year-to-year fluctuations, but the overall trajectory is clearly upward. In the earlier decades (1950s-1960s), annual maximum temperatures generally remain below 30°C, with occasional variations. From the 1970s onward, temperatures begin to rise steadily, crossing 30.5°C by the mid-1980s and exceeding 31°C in several years after 2000.

In recent decades, particularly post-2000, both the frequency and magnitude of high-temperature years increase, with several years recording basin-averaged annual maximum temperatures above 31°C. This intensification suggests not only warming but also a rising likelihood of extreme hot years.

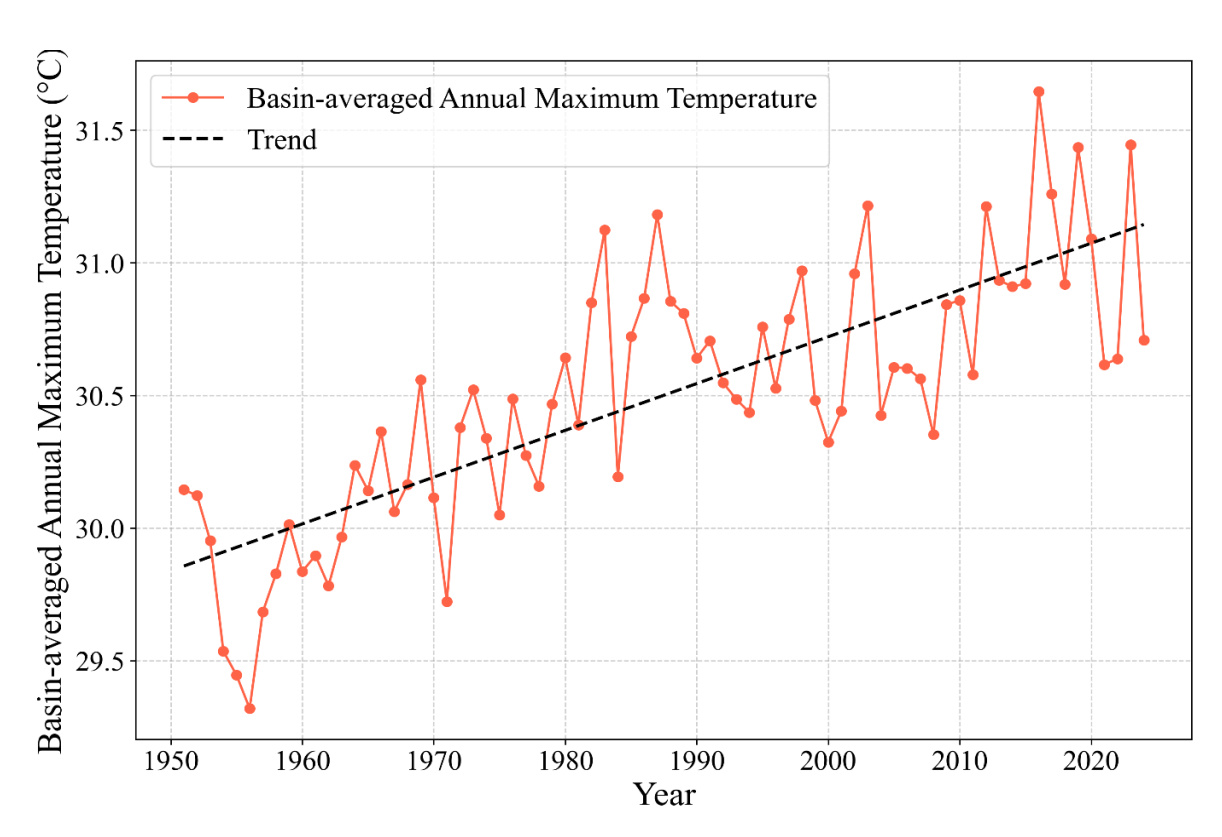


Fig. 7. Time-series of basin-averaged annual maximum temperature (°C) from 1951-2024

5. Decadal variations

5.1. Decadal mean rainfall

From the basin-averaged annual rainfall, decadal averages (1951-1960, 1961-1970, 1971-1980, 1981-1990, 1991-2000, 2001-2010, and 2011-2020), hereafter referred to as "decadal mean rainfall," were derived. The decadal mean rainfall exhibits noticeable variability, accompanied by a weak overall increasing trend from 1951-2020 (Fig. 8). Rainfall remains relatively stable between 1951 and 2020, fluctuating within a narrow range of 450-500 mm. From 1951, rainfall increases gradually until 1980, declines during 1981-1990, and then begins to rise again after 2000. The driest decade is 1981-1990, with a mean of 450.6 mm, marking a pronounced dry phase for the basin. The sharpest increase occurs in 2011-2020, when the decadal mean reaches 500.38 mm, approximately 8.92% increase relative to 1951-1960. This recent rise suggests enhanced rainfall contributions, potentially linked to more frequent extreme events, stronger monsoon activity, or shifting moisture transport patterns associated with climate variability and warming.

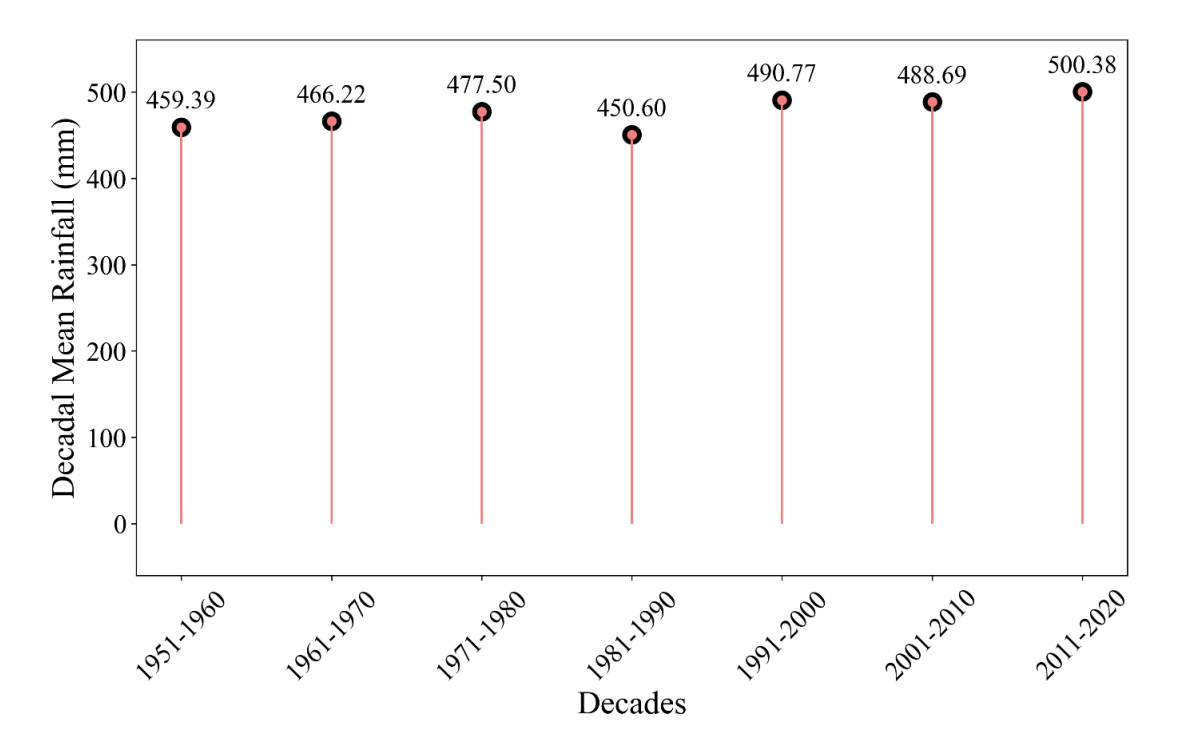


Fig. 8. Decadal mean rainfall variations in the CRB (1951-2020)

5.2. Decadal mean minimum temperature

Decadal averages of the basin-averaged annual minimum temperature were calculated for the periods 1951-1960, 1961-1970, 1971-1980, 1981-1990, 1991-2000, 2001-2010, and 2011-2020 (Fig. 9). These values are hereafter referred to as the "decadal mean minimum temperature." Decadal mean minimum temperature shows a steady warming trend across the basin from 1951-2020. During the 1951-1960 decade, the average minimum temperature was approximately 20.20°C, followed by slight fluctuations in the subsequent decades, with values remaining close to 20°C. The lowest decadal mean (19.96°C) occurred during 1971-1980, after which temperatures began to rise gradually. From the 1980s onward, each successive decade shows a marginal but consistent increase in minimum temperatures. The most recent decade (2011-2020) exhibits the highest value at 20.69°C, indicating a clear warning signal. Overall, the long-term pattern suggests that nighttime temperatures in the basin have been increasing over the last seven decades, reflecting a gradual rise in minimum temperature conditions likely associated with regional climate warming.

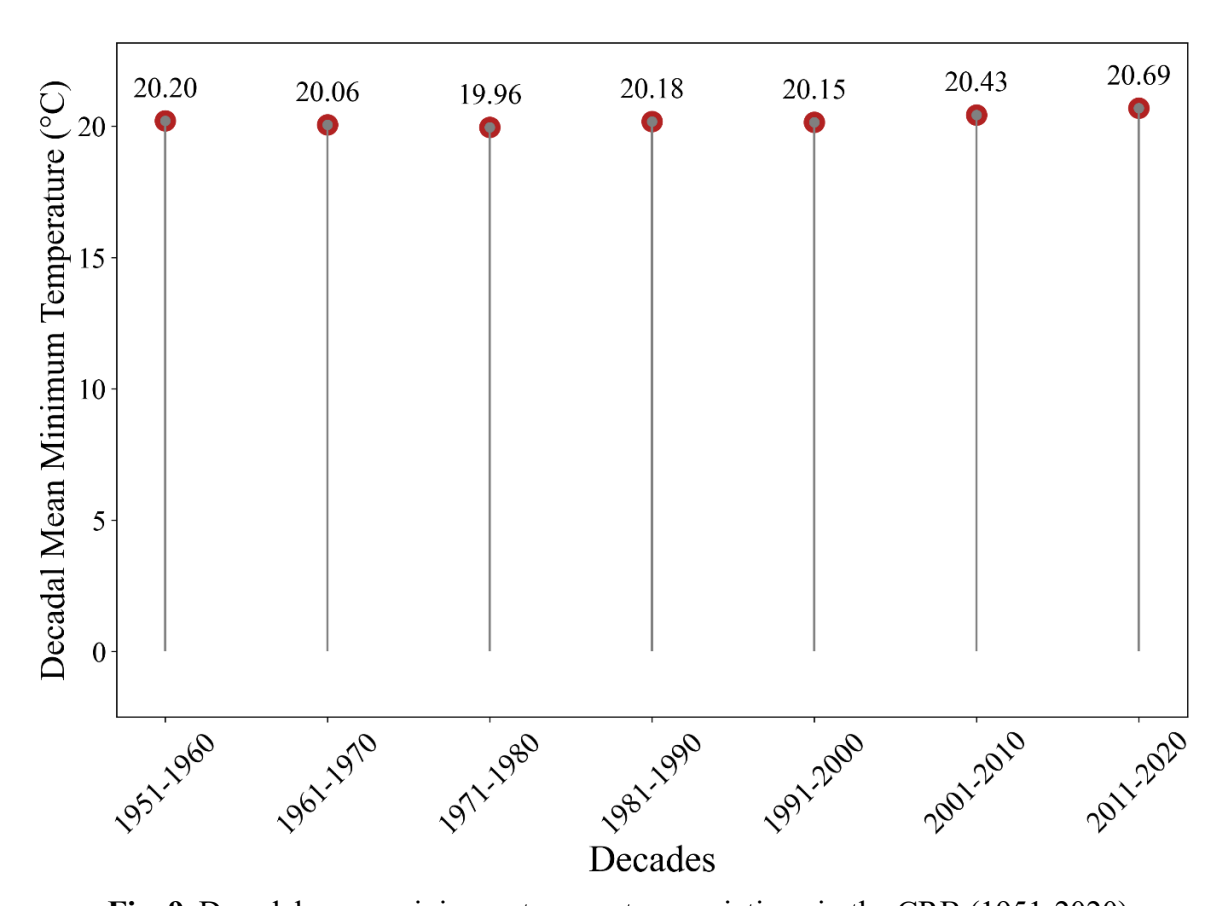


Fig. 9. Decadal mean minimum temperature variations in the CRB (1951-2020)

5.3. Decadal mean maximum temperature

Using the basin-averaged annual maximum temperature values, decadal averages were subsequently calculated for each decade (1951-1960, 1961-1970, 1971-1980, 1981-1990, 1991-2000, 2001-2010, and 2011-2020). These are hereafter referred to as the "decadal mean maximum temperature." Fig. 10 shows the decadal mean maximum temperature, revealing a clear and consistent warming pattern across the seven decades from 1951-2020. The earliest decade (1951–1960) records the lowest mean maximum temperature at about 29.79°C. In the following decades, temperatures rise gradually, reaching around 30.13°C in the 1960s and 30.30°C in the 1970s. A more pronounced increase appears from the 1980s onward, with the 1981-1990 decade showing a mean of 30.76°C. This warming trend continues into the 1990s and 2000s, where the decadal means remain consistently above 30.6°C. The highest value is observed in the most recent decade (2011-2020), reaching 31.09°C. Overall, the decadal averages indicate a steady long-term warming of more than 1°C across the basin, with the most rapid increase occurring in the recent decades.

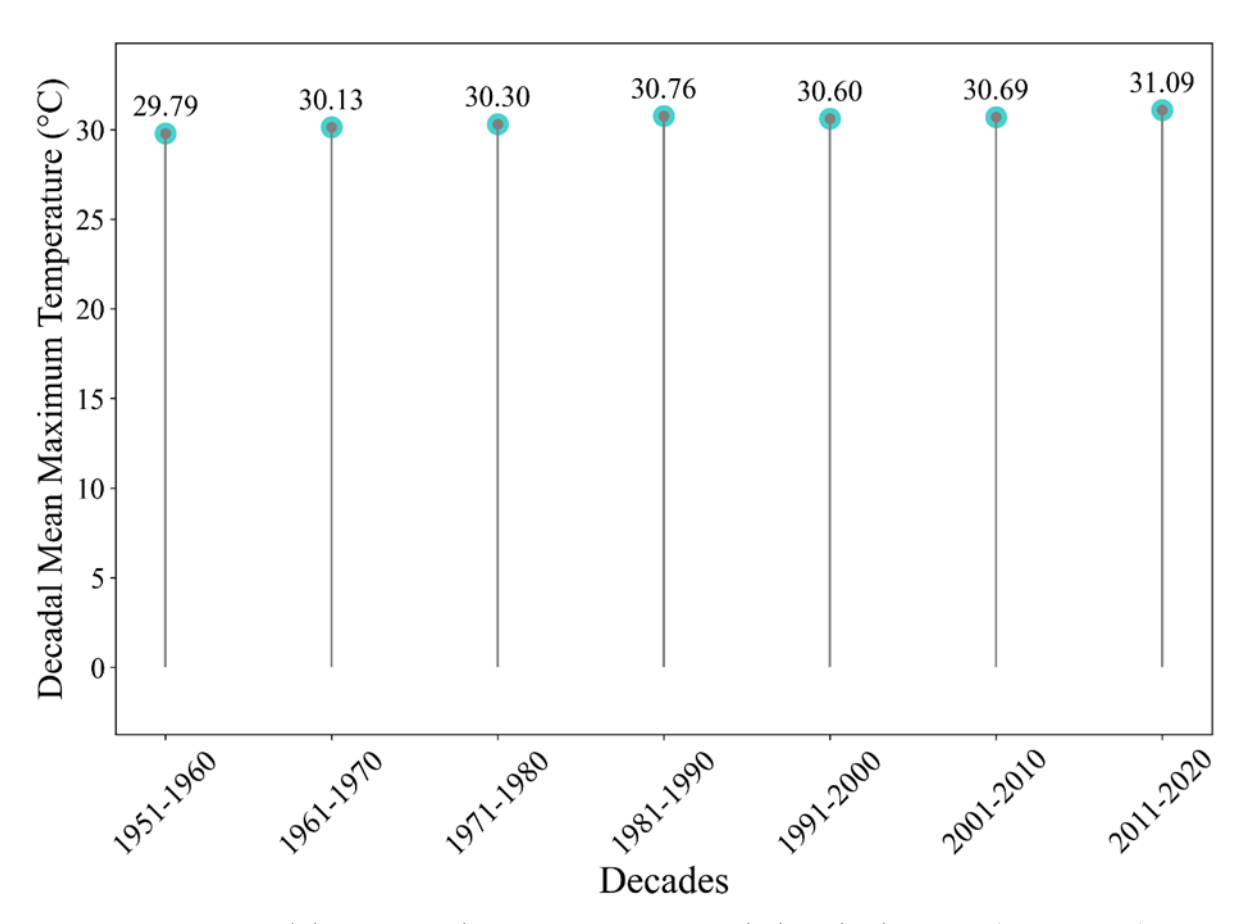


Fig. 10. Decadal mean maximum temperature variations in the CRB (1951-2020)

6. Monthly relative humidity variability across different stations

The daily relative humidity (%) dataset from CWC was available for the period 2012-2022. Fig. 11 illustrates the long-term monthly mean relative humidity for selected CWC stations within the CRB, with the corresponding stream names indicated in brackets. The complete list

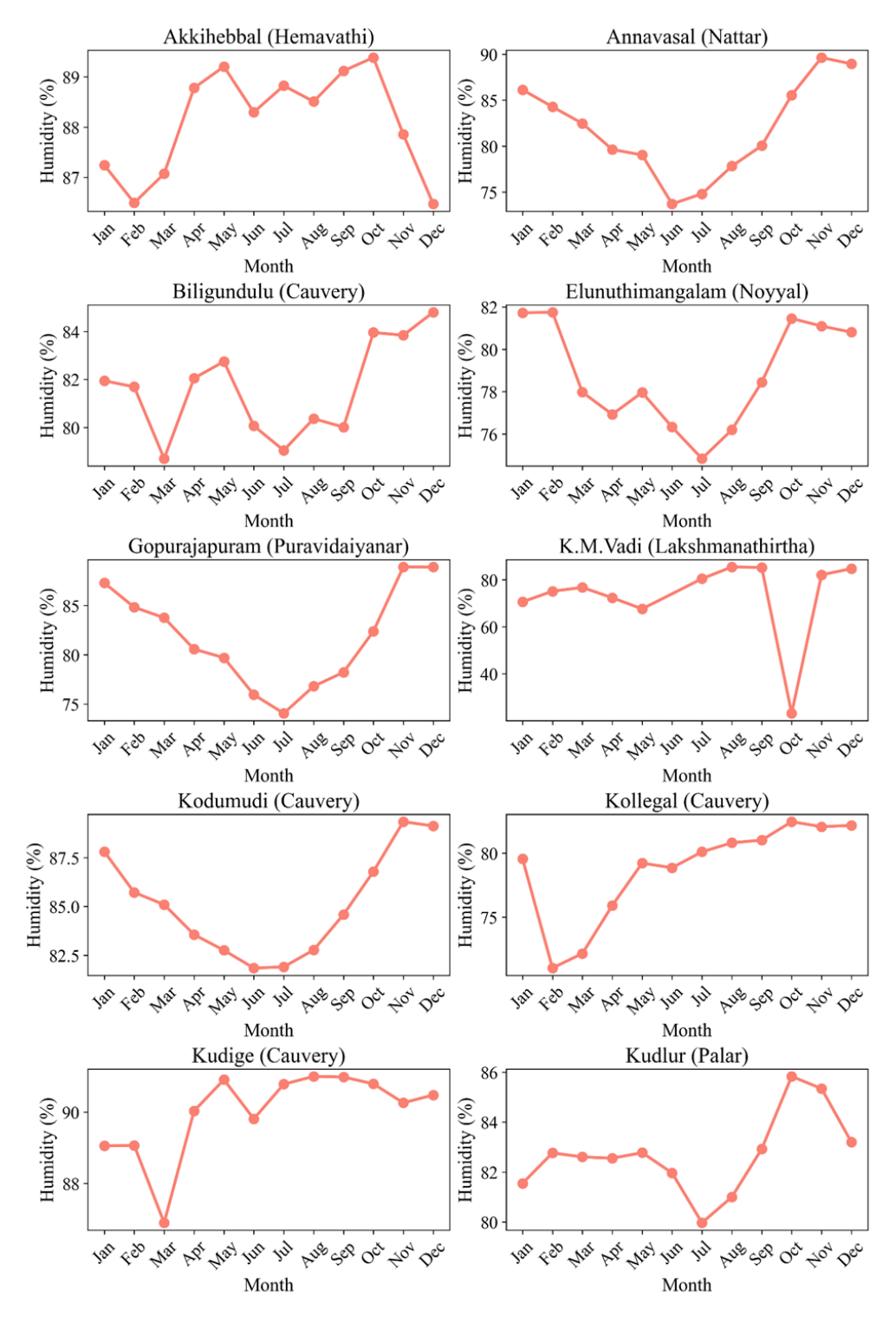


Fig. 11. Monthly variation of relative humidity (%) at selected CWC stations across the CRB (stream names in brackets)

of all stations for which relative humidity data is available is provided in Table 1. The monthly humidity patterns across the CWC stations in the CRB show a clear seasonal cycle driven by monsoon dynamics. Most stations exhibit lower humidity during the dry pre-monsoon months (January-May), except for a few locations, such as Elunuthimangalam, Gopurajapuram, and Kodumudi, which maintain relatively higher values. This is followed by a pronounced increase during the SW monsoon (June-September) and a secondary peak during the NE monsoon (October-December), particularly across the eastern parts of the basin. Upstream and western stations, such as Akkihebbal, Kudige, Kodumudi, and Kollegala, maintain relatively high humidity throughout the year due to their wetter climatic and topographic settings. In contrast, eastern stations like Annavasal, Gopurajapuram, and Elunuthimangalam exhibit pronounced summer dryness and strong post-monsoon increases. Anomalies such as the abrupt drop at K.M. Vadi likely reflect data issues rather than climatic behaviour. Overall, the station-wise humidity climatology captures the spatial and seasonal variability in atmospheric moisture that regulates evapotranspiration, soil moisture dynamics, and hydroclimatic processes across the CRB.

7. Monthly evaporation variability across different stations

Monthly evaporation (mm), derived from CWC daily data spanning 2012-2022, is shown for a few representative stations in Fig. 12, with the corresponding stream names indicated in brackets. The complete list of all CRB stations for which evaporation data are available is provided in Table 1. The variability reflects the combined influence of temperature, humidity, and monsoon conditions. Most stations experience increasing evaporation from January onward, peaking ding the hot pre-monsoon months (March-May) when high temperatures and low humidity promote maximum evaporative losses. Evaporation declines sharply with the onset of the SW monsoon (June-September), reflecting increased cloud cover, reduced solar radiation, and higher humidity. A secondary rise is observed at a few stations during the postmonsoon transition (October-November), particularly in upstream and western sub-basins such as Kollegala, Kudige, and M.H. Halli, where clearer skies and warmer conditions persist briefly after the monsoon withdrawal. Downstream stations, such as Musiri, Nallamaranpatty, and Annavasal, exhibit smoother seasonal cycles with pronounced pre-monsoon peaks and lower values during the monsoon months. Overall, the station-wise variability highlights the influence of local climate, topography, and sub-basin hydro-climatology on evaporation dynamics across the CRB.

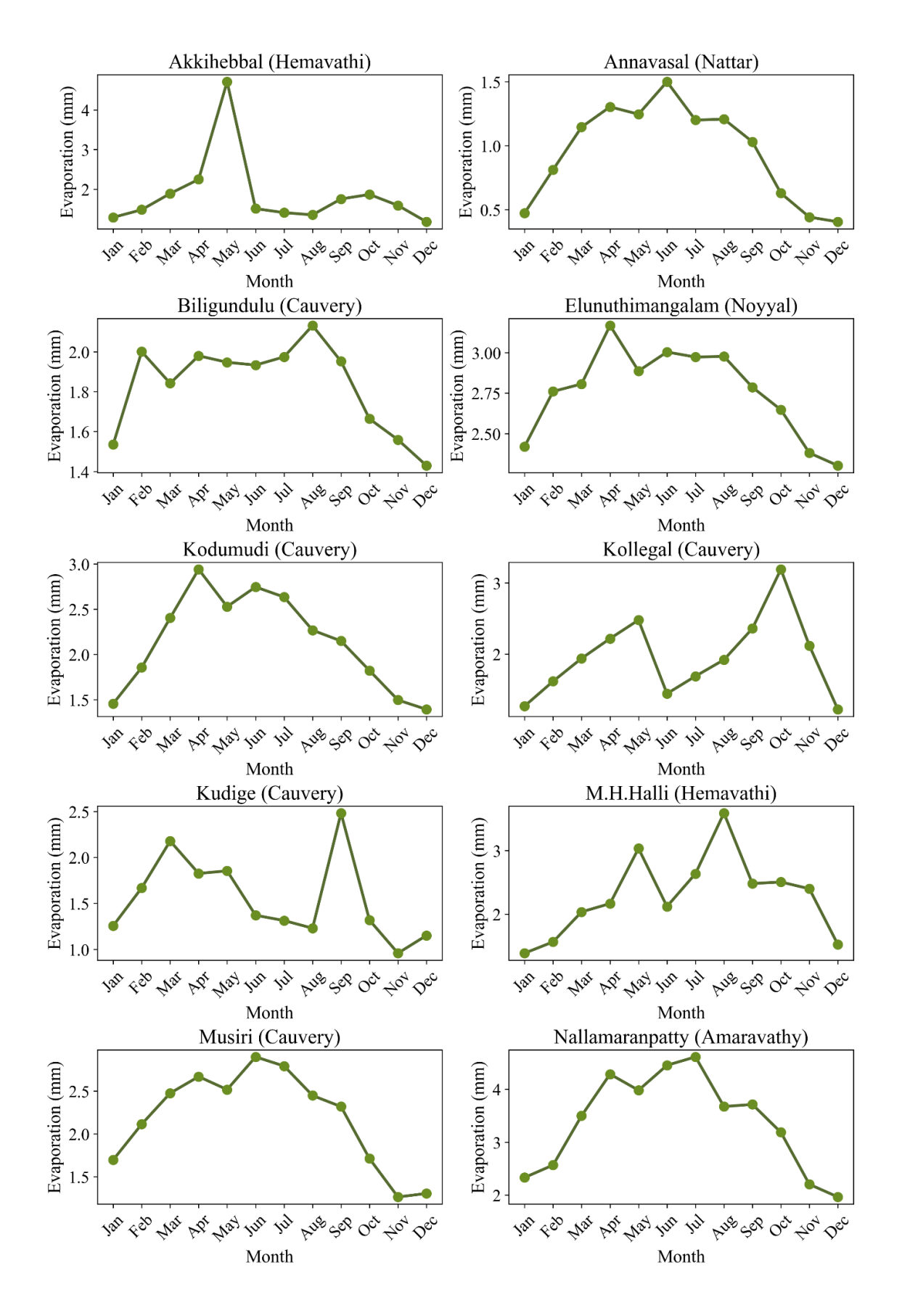


Fig. 12. Monthly variation of evaporation (mm) at selected CWC stations across the CRB (stream names in brackets)

8. Monthly wind velocity variability across different stations

The long-term monthly mean wind velocity (km/h), derived from daily CWC observations for 2012-2022, exhibits a clear and consistent seasonal pattern across stations in the CRB (Fig. 13). For clarity, Fig. 13 presents only a subset of representative stations, with the corresponding stream names indicated in brackets. The complete list of all stations for which wind data are available is provided in Table 1. Wind speeds generally remain low during the winter months (December-February), rise gradually during the pre-monsoon period, and reach their peak during the SW monsoon season (June-August). This behaviour aligns strongly with the seasonal evolution of the regional monsoon circulation, where increasing temperature gradients and monsoonal flows enhance wind activity across southern India. The post-monsoon months (September-October) exhibit a rapid decline, marking the transition to calmer atmospheric conditions.

While the overall seasonal cycle is broadly similar, the magnitude and sharpness of wind velocity changes vary substantially across stations, reflecting the influence of basin topography and local environmental conditions. Stations such as Biligundulu, Kollegal, and Elunuthimangalam exhibit relatively higher peak wind velocities during the monsoon season, indicating greater exposure to open terrain and valley-driven airflow. Conversely, stations like Gopurajapuram, Kudige, and Annavasal show lower amplitudes and smoother variations throughout the year, suggesting sheltered conditions and reduced sensitivity to large-scale synoptic flows. These spatial differences highlight the complex interplay between regional climate forces and local physiographic controls.

The data strongly reveal the dominance of the SW monsoon in shaping the wind climatology of the CRB. At most stations, winds strengthen markedly from May onward, peak between June and August, and weaken sharply after September. However, certain stations outside the core Cauvery region demonstrate distinct behaviour. For example, Kudlur shows relatively weak winds during the SW monsoon but exhibits an anomalous peak in December, likely reflecting the influence of NE monsoon flows and terrain channelling in the Palar valley. These contrasts illustrate basin-specific wind regimes governed by differing topographic exposures and seasonal wind systems.

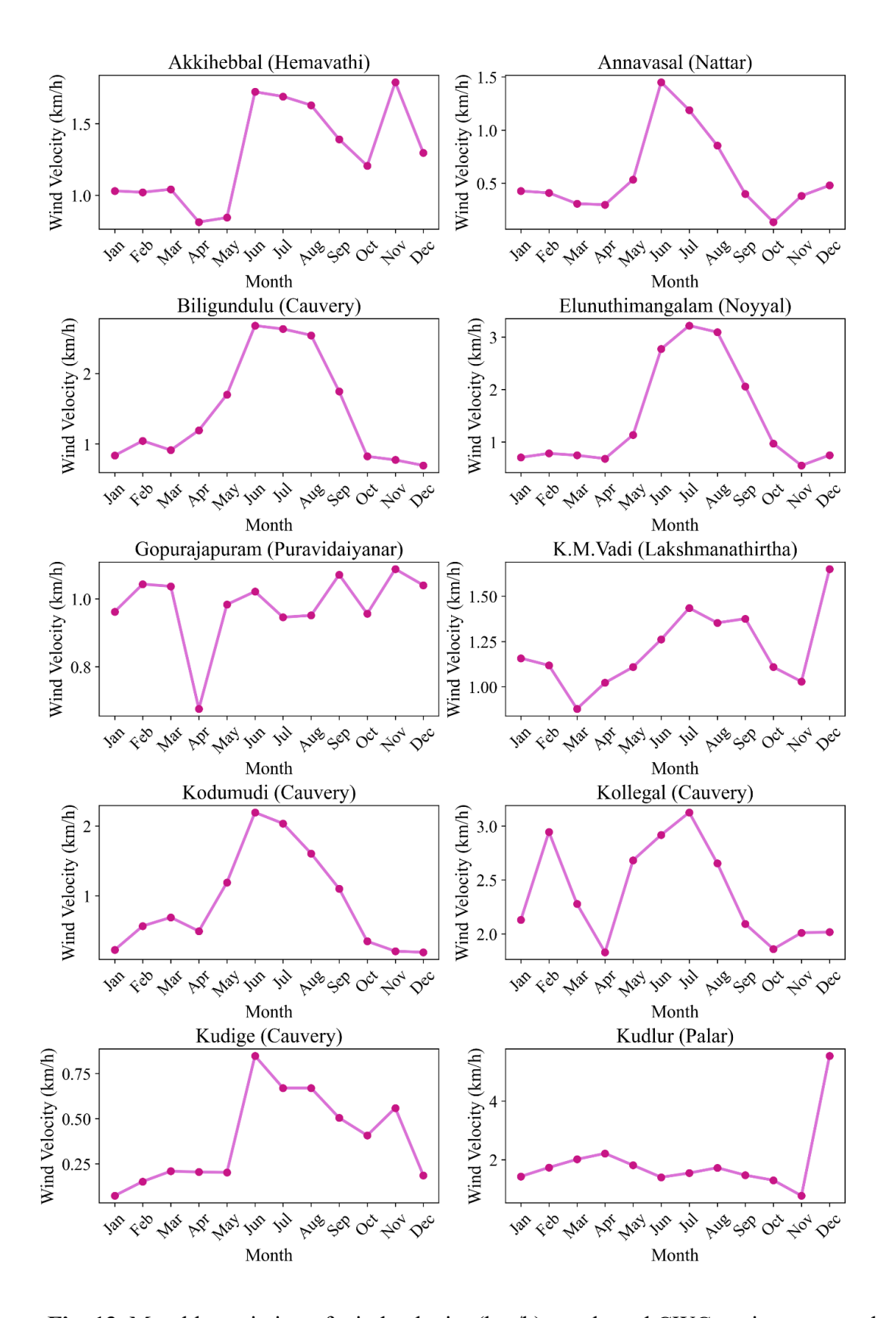


Fig. 13. Monthly variation of wind velocity (km/h) at selected CWC stations across the CRB (stream names in brackets)

9. Bias-corrected climate projections from CMIP6 models

Bias-corrected climate projections from three CMIP6 models, EC-Earth3, MPI-ESM1-2-HR, and MRI-ESM2-0, were obtained from Mishra et al. (2020) at a spatial resolution of 0.25°. These models were selected because they are among the best-performing in reproducing the Indian Summer Monsoon, rainfall seasonality, and temperature variability. Their advanced physical parameterizations, higher spatial resolution, and demonstrated ability to capture monsoon teleconnections and hydroclimatic extremes make them particularly suitable for climatological analysis of the CRB. The detailed specifications of these models are provided in Table 2.

Table 2. Description of models used for future climate projections

S. No.	Model	Institute	Native Resolution	Vertical levels	Reference
1	EC-Earth3	EC-Earth- Consortium, Europe	1°	T255L91 (~1°)	Doscher et al. (2021)
2	MPI-ESM1-2-HR	Max Planck Institute for Meteorology (MPI), Germany	0.4°	T127 (0.93°)	Muller et al. (2018)
3	MRI-ESM2-0	Meteorological Research Institute (MRI), Japan	1.125° × 1.125°	80 levels; top level 0.01 hPa	Zanis et al. (2022)

9.1. Rainfall future projections

Daily bias-corrected rainfall projections for each SSP were first aggregated to obtain annual rainfall totals. Subsequently, the ensemble mean of annual rainfall from all three models was calculated for each scenario. Fig. 14 illustrates the ensemble mean annual rainfall over the CRB for the period 2015-2100, derived from three bias-corrected CMIP6 models. For each SSP, the

ensemble mean reflects the central tendency of the model outputs, while the shaded bands represent the inter-model spread (minimum to maximum), capturing the associated uncertainty across models.

Across all four SSPs, SSP126 (low emissions), SSP245 (medium stabilisation), SSP370 (high intermediate), and SSP585 (very high emissions), the ensemble mean annual rainfall shows substantial year-to-year variability throughout the 21st century. No strong or persistent monotonic trend is apparent in any scenario, although SSP370 and SSP585 display slightly more frequent high-rainfall years toward the end of the century, suggesting a possibility of intensifying extremes under higher warming levels.

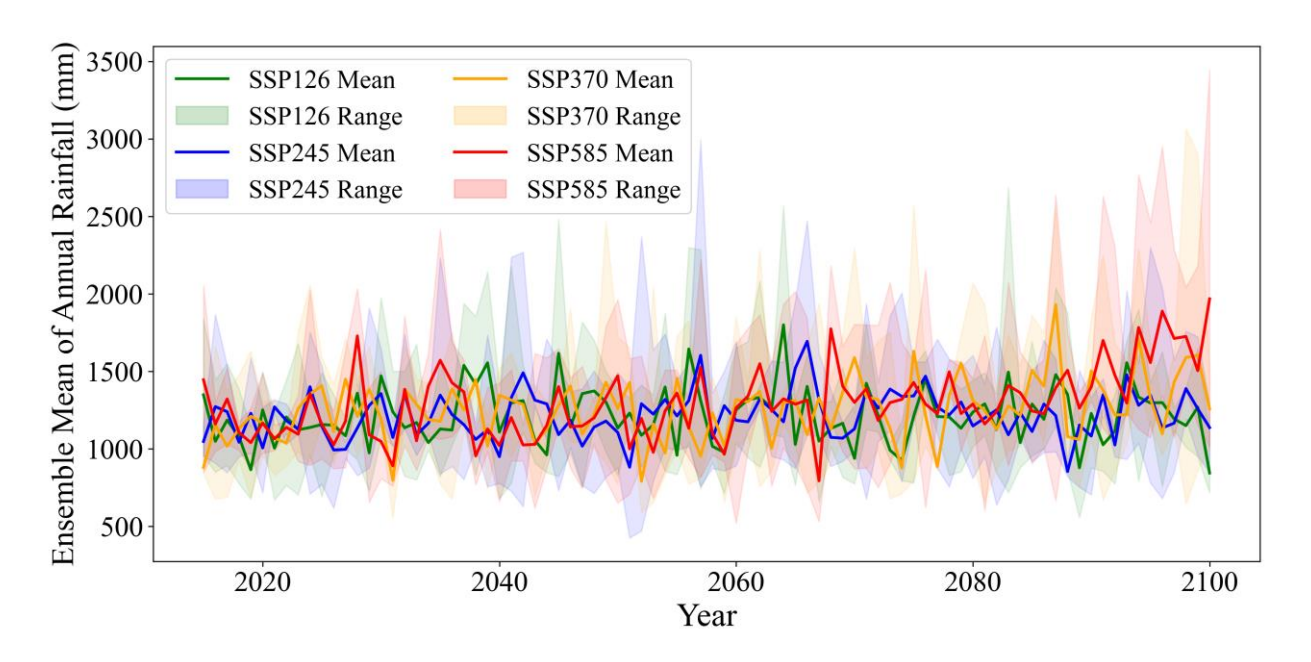


Fig. 14. Ensemble mean of annual rainfall (2015-2100) over the CRB under various biascorrected CMIP6 SSP scenarios

The ensemble spread (shaded areas) remains considerable across all pathways, indicating large model-to-model differences in simulating annual rainfall over the CRB. This uncertainty widens toward the latter decades of the century, particularly under the higher-emission scenarios (SSP370 and SSP585), implying greater divergence among models in a warmer climate. Despite this, the multi-model means of SSP126, SSP245, and SSP370 remain broadly similar for much of the century, with SSP585 showing a slight upward shift after ~2080.

Overall, the projections indicate that, while the ensemble mean annual rainfall may not change drastically across scenarios, internal climate variability and model uncertainty dominate the future signal. Higher-emission scenarios may, however, be associated with an increased

likelihood of extreme wet years, highlighting the need to prepare for enhanced rainfall variability rather than large shifts in long-term means.

9.2. Minimum temperature future projections

The annual mean was calculated from daily bias-corrected minimum temperature projections for each SSP. Subsequently, the ensemble mean of annual minimum temperature across all three models was computed for each scenario. Fig. 15 presents the ensemble mean annual minimum temperature over the CRB for the period 2015-2100, based on three bias-corrected CMIP6 models. For each SSP, the ensemble mean represents the central tendency of the model outputs, while the shaded bands indicate the inter-model range (minimum to maximum), illustrating the uncertainty across models.

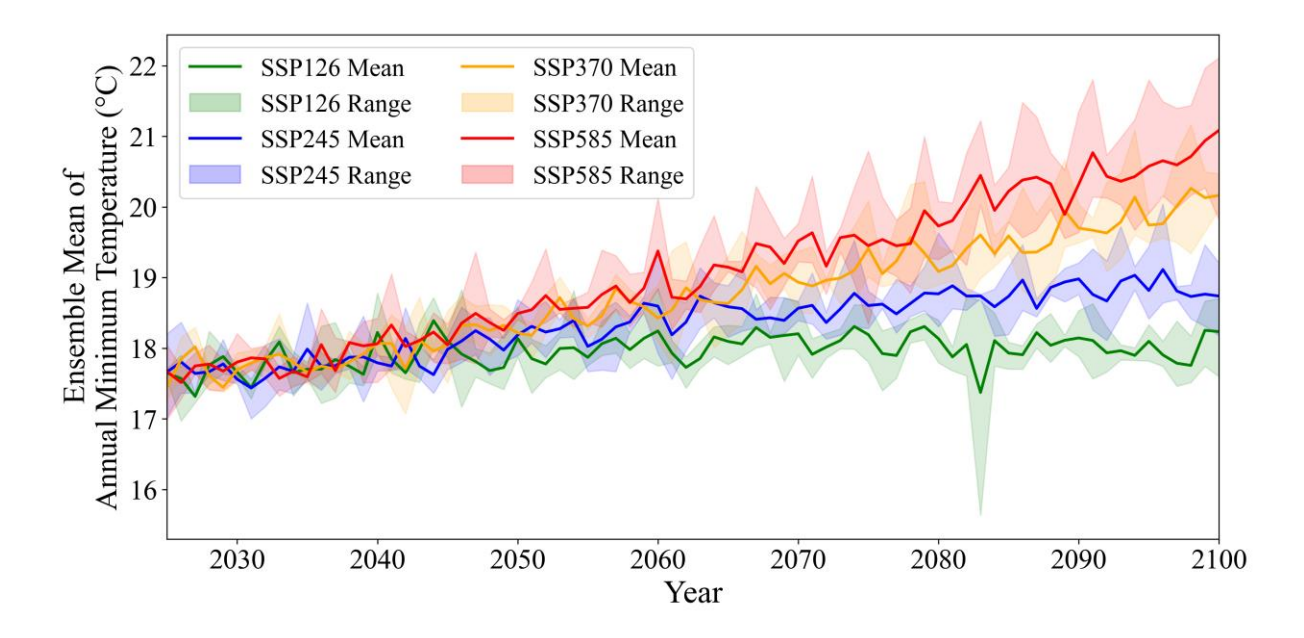


Fig. 15. Ensemble mean of annual minimum temperature (2015-2100) over the CRB under various bias-corrected CMIP6 SSP scenarios

The ensemble mean annual minimum temperature over the CRB exhibits a clear and persistent warming trend across all CMIP6 SSP scenarios from 2015 to 2100. Although the overall direction of change is consistent, the magnitude of warming varies depending on the emission pathway. Under SSP126 (green), which represents strong mitigation and lower radiative forcing, temperatures rise gradually and tend to stabilize toward the end of the century, reaching slightly above 18°C. SSP245 (blue) indicates a moderate warming trajectory, with values increasing to around 19°C by 2100. In contrast, SSP370 (orange) shows a more

pronounced increase, with end-century values approaching 20°C. The strongest warming occurs under SSP585 (red), where temperatures exceed 21°C by late century, highlighting the consequences of a high-emission future. Notably, the uncertainty band (spread between the minimum and maximum model values) widens toward the end of the century, especially in the higher-emission scenarios.

9.3. Maximum temperature future projections

The annual mean was derived from daily bias-corrected maximum temperature projections for each SSP. The ensemble mean of annual maximum temperature from all three models was then calculated for each scenario. Fig. 16 displays the ensemble mean of annual maximum temperature over the CRB for the period 2015-2100, based on three bias-corrected CMIP6 models. For each SSP, the ensemble mean represents the overall tendency of the projection models, while the surrounding shaded bands show the full range of inter-model outputs, from minimum to maximum, highlighting the associated uncertainty and variability (Fig. 16). The figure illustrates the evolution of ensemble mean of annual maximum temperatures from 2020 to 2100 across four SSPS, temperatures rise gently from roughly 27°C to about 28-29°C by the end of the century, accompanied by a relatively tight spread that signals strong agreement among models and reflects the influence of robust mitigation strategies. SSP245 shows a steadier warming pattern, reaching slightly above 28°C by 2100 with a moderate level of variability, consistent with its characterization as an intermediate development pathway. SSP370 produces more pronounced warming, with values nearing or surpassing 29°C later in the century and a broader envelope that indicates increasing divergence among model outputs under intensified emissions. SSP585 demonstrates the strongest warming signal, ~30°C as the century progresses, and shows the widest range of projections, characteristic of a fossil-fuelintensive trajectory.

Overall, the higher-emission pathways yield steeper temperature increases and greater uncertainty, while the lower-emission scenarios result in more restrained warming with closer model agreement, underscoring how emissions choices shape both expected outcomes and the spread of potential futures.

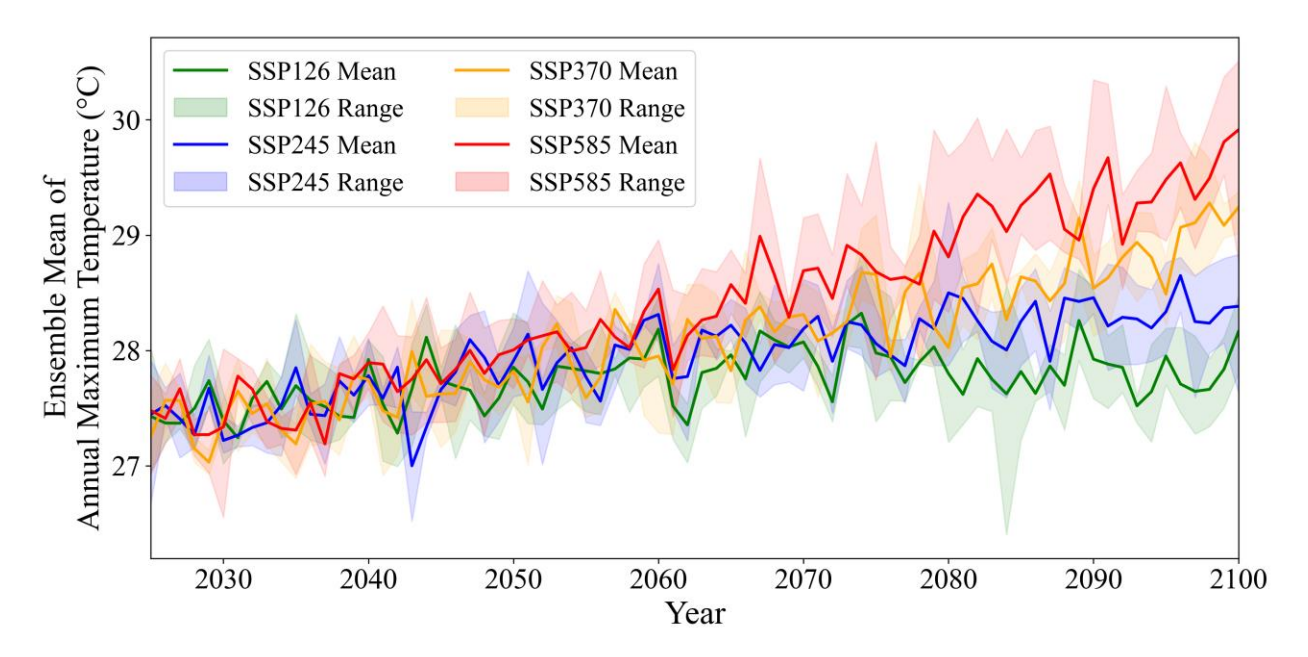


Fig. 16. Ensemble mean of annual maximum temperature (2015-2100) over the CRB under various bias-corrected CMIP6 SSP scenarios

10. Past drought & flood incidents in the CRB

CRB has experienced several major hydroclimatic extremes over the past decade, reflecting its high sensitivity to monsoon variability and extreme rainfall events.

1. 2016-2017 drought in Tamil Nadu

In 2016-17, parts of the Cauvery Basin in Tamil Nadu experienced one of the worst droughts in over a century, following a dramatic failure of the NE monsoon. Seasonal rainfall deficits reached up to ~62% below normal, reservoirs fell to very low levels, and irrigation water from the river and upstream releases was insufficient. The drought had severe repercussions on agriculture, resulting in widespread crop losses and distress among farmers. The crisis contributed to large-scale protests by farmers demanding relief and loan waivers (https://en.wikipedia.org/wiki/2016%E2%80%932017 Drought in Tamil Nadu).

2. 2015 flood in Tamil Nadu and Puducherry

The 2015 South India floods were caused by exceptionally heavy NE monsoon rains that severely affected Tamil Nadu, Andhra Pradesh, and Puducherry, with Chennai experiencing the worst impacts. Over 500 people died and more than 1.8 million were displaced, resulting in major economic losses. The disaster was intensified by poor

urban planning and inadequate drainage infrastructure (https://en.wikipedia.org/wiki/2015 South India floods).

3. 2018 flood event in Kodagu, Karnataka

In 2018, the upstream part of the CRB, especially Kodagu district in Karnataka, recorded unusually heavy rainfall during the monsoon. Between June 1 and August 16, rainfall totals were significantly above normal (about 41% higher than typical for that period), marking one of the wettest monsoons since 1994 (https://www.newindianexpress.com/states/karnataka/2018/Aug/19/kodagu-sees-highest-monsoon-rain-since-1994-1859630.html).

4. 2019 flash floods and crop loss in Karnataka

During 2019, erratic rainfall during the monsoon, including prolonged dry spells followed by intense downpours, caused a combination of drought-like conditions (early in the season) and flash floods (later). This pattern damaged about 25% of the kharif (summer) crop across several districts in Karnataka (https://scroll.in/article/939302/driven-by-climate-change-erratic-rain-destroyed-25-of-crops-in-karnatakas-cauvery-basin-this-year).

5. 2023 drought in Karnataka

Recently, in 2023, Karnataka endured its worst drought in 123 years, with both the southwest and northeast monsoons failing, and 223 out of 236 taluks declared drought-hit. The state recorded only 642 mm of rainfall, compared to the normal 852 mm, causing reservoir levels to drop sharply, widespread crop failures, and a steep decline in food-grain production (from the expected 148 lakh tonnes to around 80 lakh tonnes). As a result, many farmers lost their livelihoods, and cattle fodder vanished (https://www.newindianexpress.com/states/karnataka/2023/Dec/25/drought-year-for-karnataka-farmers-people-face-distress-2644645.html).

These historical events underscore the vulnerability of the CRB to rainfall extremes. Such pronounced fluctuations, ranging from prolonged dry spells to intense monsoon downpours, have caused widespread agricultural losses, water scarcity, and socioeconomic distress across the basin. These recurrent climate-driven hazards highlight the critical need for comprehensive studies to understand long-term hydroclimatic variability and to inform adaptive water management, disaster preparedness, and climate resilience strategies in the CRB.

11. Summary and recommendations

This report provides a comprehensive assessment of the historical and future climatic behaviour of the CRB using long-term observational datasets and state-of-the-art CMIP6 bias-corrected climate projections. Analyses of rainfall, minimum temperature, maximum temperature, relative humidity, evaporation, and wind velocity reveal clear patterns of spatial heterogeneity and evolving climatic signals across the basin. Historical IMD records from 1951-2024 indicate a modest but statistically significant increase in basin-averaged annual rainfall, accompanied by substantial interannual variability and intensified extremes in recent decades. Minimum and maximum temperatures show strong and consistent warming trends, with the most rapid rise occurring after the mid-1990s, reflected in the emergence of hotspots in the southeastern parts of the basin. Evaporation, humidity, and wind velocity exhibit distinct seasonal patterns governed by monsoon dynamics and local physiography.

Future climate projections under four bias-corrected CMIP6 SSP scenarios indicate continued warming throughout the 21st century. While rainfall projections do not show strong long-term shifts, higher-emission scenarios exhibit greater variability and an increased likelihood of extreme wet years. Temperature projections show robust warming under all pathways, with the magnitude of increase strongly dependent on the emission scenario. Maximum and minimum temperature projections consistently point to intensified thermal stress by late century, particularly under SSP370 and SSP585. Together, these findings highlight a future characterized more by increased climatic variability and thermal intensification than by large shifts in mean rainfall.

Further, findings highlight the need for a more climate-resilient approach to managing water resources across the CRB. Rising temperatures and increasing rainfall variability necessitate adaptive reservoir operations, expanded groundwater recharge initiatives, and enhanced coordination between surface and groundwater use. At the same time, the projected intensification of heatwaves and droughts underscores the importance of basin-wide preparedness through early-warning systems, heat action plans, and agricultural practices that conserve water. Although long-term rainfall trends show only modest changes, the growing occurrence of extreme rainfall years, particularly under high-emission scenarios, suggests a heightened risk of flooding. Addressing this requires strengthened stormwater infrastructure, improved hydrological monitoring, and stricter enforcement of floodplain regulations. Agriculture must also adapt to a warmer and drier environment through crop diversification,

the development of climate-tolerant varieties, revised sowing calendars, and increased adoption of micro-irrigation. Enhancing the observational network is equally crucial; expanding and modernizing IMD and CWC stations, especially in sensitive areas, will help capture finer-scale climatic variability and support more robust modelling. Long-term planning for cities, water systems, and inter-state water-sharing arrangements should incorporate climate projections and consider multiple future scenarios to improve resilience. Finally, transitioning toward lower-emission development pathways can significantly reduce future warming and associated risks, making mitigation efforts a critical component of safeguarding the basin's water and agricultural sectors.

12. Significance of the climatological profile of the CRB

This report is significant because it provides one of the most detailed and integrated assessments of past and future climate variability in the CRB, a region of major ecological, agricultural, and socio-economic importance. By combining seven decades of high-resolution observational data with advanced CMIP6 projections, it offers a holistic understanding of how key hydroclimatic variables are evolving in response to regional and global climate change. The report highlights critical shifts in temperature, rainfall variability, and atmospheric moisture dynamics that directly influence water availability, agricultural productivity, and ecological stability in the basin.

Moreover, its synthesis of historical trends and future scenarios offers actionable insights for policymakers, water managers, and planners. The analysis not only quantifies emerging risks, such as intensifying heat stress and rainfall extremes, but also provides a scientific basis for climate-resilient decision-making. By identifying hotspots, documenting long-term trends, and highlighting uncertainties, the report strengthens the foundation for sustainable water governance, climate adaptation strategies, and inter-state resource management in the CRB.

References

- 1. Cauvery Basin Report, Central Water Commission, Ministry of Water Resources and National Remote Sensing Centre, ISRO, Department of Space, Govt. of India.
- 2. Döscher, R., Acosta, M., Alessandri, A., Anthoni, P., Arneth, A., Arsouze, T., Bergmann, T., Bernadello, R., Bousetta, S., Caron, L.P. and Carver, G., 2021. The EC-

- earth3 Earth system model for the climate model intercomparison project 6. Geoscientific Model Development Discussions, 2021, pp.1-90.
- 3. Ghosh, N., Bandyopadhyay, J. and Thakur, J., 2018. Conflict over Cauvery waters: Imperatives for innovative policy options. New Delhi, India: Observer Research Foundation.
- 4. Gouda, K.C., Nikhilasuma, P., Benke, M. and Agnihotri, G., 2024. Assessment of rainfall variability over Karnataka state in India. Natural Hazards Research, 4(2), pp.246-254.
- 5. Mishra, V., Bhatia, U. and Tiwari, A.D., 2020. Bias-corrected climate projections for South Asia from the Coupled Model Intercomparison Project-6. Scientific Data, 7(1), p.338.
- 6. Müller, W.A., Jungclaus, J.H., Mauritsen, T., Baehr, J., Bittner, M., Budich, R., Bunzel, F., Esch, M., Ghosh, R., Haak, H. and Ilyina, T., 2018. A higher-resolution version of the max planck institute earth system model (MPI-ESM1. 2-HR). Journal of Advances in Modeling Earth Systems, *10*(7), pp.1383-1413.
- 7. SK, A.R., Panday, D.P. and Kumar, M., 2023. Decoding the enigma of 100-year record-breaking rainfall over Tamil Nadu using wavelet analysis. Groundwater for Sustainable Development, 23, p.101007.
- 8. Sushant, S., Balasubramani, K. and Kumaraswamy, K., 2015. Spatio-temporal analysis of rainfall distribution and variability in the twentieth century, over the Cauvery Basin, South India. In Environmental management of river basin ecosystems (pp. 21-41). Cham: Springer International Publishing.
- 9. Zanis, P., Akritidis, D., Turnock, S., Naik, V., Szopa, S., Georgoulias, A.K., Bauer, S.E., Deushi, M., Horowitz, L.W., Keeble, J. and Le Sager, P., 2022. Climate change penalty and benefit on surface ozone: a global perspective based on CMIP6 earth system models. Environmental Research Letters, 17(2), p.024014.
- 10. The New Indian Express. (2018, August 19). Kodagu sees highest monsoon rain since 1994. Retrieved September 05, 2025, from https://www.newindianexpress.com/states/karnataka/2018/Aug/19/kodagu-sees-highest-monsoon-rain-since-1994-1859630.html
- 11. Scroll Staff. (2019, September 4). Driven by climate change, erratic rain destroyed 25% of crops in Karnataka's Cauvery basin this year. Retrieved November 26, 2025, from https://scroll.in/article/939302/driven-by-climate-change-erratic-rain-destroyed-25-of-crops-in-karnatakas-cauvery-basin-this-year

- 12. The New Indian Express. (2023, December 25). Drought year for Karnataka, farmers, people face distress. Retrieved October 26, 2025, from https://www.newindianexpress.com/states/karnataka/2023/Dec/25/drought-year-for-karnataka-farmers-people-face-distress-2644645.html
- 13. Wikipedia. 2016-2017 Drought in Tamil Nadu. Retrieved September 15, 2025, from https://en.wikipedia.org/wiki/2016%E2%80%932017 Drought in Tamil Nadu
- 14. Wikipedia. 2015 South India floods. Retrieved August 01, 2025, from https://en.wikipedia.org/wiki/2015 South India floods

Back cover page





© cCauvery, cGanga and NRCD, 2024